In Vitro Cytotoxicity of Oxide Nanoparticles: Comparison to Asbestos, Silica, and the Effect of Particle Solubility †

ARTICLE *in* ENVIRONMENTAL SCIENCE AND TECHNOLOGY · AUGUST 2006

Impact Factor: 5.33 · DOI: 10.1021/es052069i · Source: PubMed

8 AUTHORS, INCLUDING:

Peter Wick
Empa - Swiss Federal Laboratories for Materi…
97 PUBLICATIONS **3,900** CITATIONS
SEE PROFILE

Robert N Grass
ETH Zurich
115 PUBLICATIONS **4,179** CITATIONS
SEE PROFILE

Ludwig K Limbach
BIOTRONIK SE & Co.KG
25 PUBLICATIONS **2,923** CITATIONS
SEE PROFILE

Arie Bruinink
Empa - Swiss Federal Laboratories for Materi…
131 PUBLICATIONS **3,179** CITATIONS
SEE PROFILE

Environ. Sci. Technol. **2006**, *40,* 4374−4381

In Vitro Cytotoxicity of Oxide Nanoparticles: Comparison to Asbestos, Silica, and the Effect of Particle Solubility†

TOBIAS J. BRUNNER,‡ PETER WICK,§ PIUS MANSER,§ PHILIPP SPOHN,§ ROBERT N. GRASS,‡ LUDWIG K. LIMBACH,‡ ARIE BRUININK,§ AND WENDELIN J. STARK*,‡

Institute for Chemical and Bioengineering, Department of Chemistry and Applied Biosciences, ETH Zurich, CH-8093 Zurich, Switzerland, and Laboratory for Biocompatible Materials, EMPA Materials Science and Technology, Lerchenfeldstrasse 5, CH-9014 St. Gallen, Switzerland

Early indicators for nanoparticle-derived adverse health effects should provide a relative measure for cytotoxicity of nanomaterials in comparison to existing toxicological data. We have therefore evaluated a human mesothelioma and a rodent fibroblast cell line for in vitro cytotoxicity tests using seven industrially important nanoparticles. Their response in terms of metabolic activity and cell proliferation of cultures exposed to 0−30 ppm nanoparticles (μg g^{-1}) was compared to the effects of nontoxic amorphous silica and toxic crocidolite asbestos. Solubility was found to strongly influence the cytotoxic response. The results further revealed a nanoparticle-specific cytotoxic mechanism for uncoated iron oxide and partial detoxification or recovery after treatment with zirconia, ceria, or titania. While in vitro experiments may never replace in vivo studies, the relatively simple cytotoxic tests provide a readily available pre-screening method.

Introduction

Over the past decade the ability to engineer and produce materials at the nano or near-atomic scale has triggered rapid product development due to their new interesting properties that were not previously seen at scales above the micrometer. Industrial applications using nanoparticles have resulted in an almost exponentially growing demand for nanosized materials. Humans are therefore increasingly exposed to such nanomaterials, beyond personnel working at production sites, since nanoparticles are now applied in a series of consumer goods (*1*−*5*). The urgency to explore the toxicological impact and the development of early indicators to detect possible adverse health effects arising from the application of nanomaterials is most evident. While classical chemical compounds are routinely subjected to well-established toxicity tests prior to release to the public, no such procedures currently exist for nanomaterials. The proactive development of nanomaterial-based products should include simple pre-screening tests. We therefore evaluated an in vitro setup based on rodent or human cells (mesothelioma MSTO-211H and rodent 3T3 fibroblast cells) as possible early toxicity indicators. Earlier toxicological studies already used similar cell lines and therefore provide a good basis for comparison (*6*−*9*). As a measure for modification of cell functionality ("cytotoxicity") two different parameters (i.e., mean cell culture activity and DNA content) were chosen. The mean cell culture activity provides a measure of the cells' overall activity and is an indicator for stress, toxic effects targeting metabolic pathways, and overall viability. The DNA content is a measure for the number of cells and gives information on the cell proliferation. To study a broad yet representative range of materials, the present study included highly insoluble ceramic materials such as ceria, titania, and zirconia, slightly soluble materials such as zinc or iron oxide, and tricalcium phosphate nanoparticles for their rapidly growing industrial applications. Silica and titania nanoparticles were included for comparison to earlier studies (*7*, *10*−*12*) and as a negative reference in the case of amorphous silica which has been used as a food additive (rheological enhancer, anti-packing-agent, generally recognized as safe by the FDA) for over 50 years. Titania and zinc oxide are used on a large scale in pigments, in sun screens, and in polymers or tires as stabilizers. Tricalcium phosphate is a prominent biomaterial for orthopedic implants (*13*) and generally considered fully biocompatible (*14*). Surface-coated iron oxide has been repeatedly proposed for medical treatments such as magnetic drug targeting systems (*15*−*19*) or as a contrast agent in magnetic resonance imaging (*20*, *21*). Zirconia and ceria are rapidly growing ceramic nanoparticulate materials with broad applications in catalysis and polishing, and as additives in polymers and dental materials (*1*, *22*, *23*). The inclusion of highly toxic crocidolite asbestos (*6*) and nontoxic silica particles allows a comparison of the effect of a series of nanomaterials referring to well-established references.

Materials and Methods

General Experimental Design. As-prepared nanoparticles (see Supporting Information for details on preparation and analysis) were dispersed in ultrapure water by sonication and thoroughly characterized for mass-mean primary particle diameter, full particle size distribution, mean number of primary particles per hard agglomerate, and content of particle agglomerates above 200 nm size. The resulting dispersions of about 1 mg of particles per mL were diluted with cell culture medium prior to experiment. Cytotoxicity of a series of oxide nanoparticles to selected human or rodent cells (see Supporting Information for details) was tested using two different assays: The total cell culture activity was spectroscopically measured as the total mitochondrial activity using the selective conversion of a formazan-type dye from its leukoform to the active dye (MTT test, see Supporting Information for details) (*24*). The total DNA content of cells is a measure for cell proliferation and can be quantified spectroscopically after converting DNA with an intercalating dye into a highly fluorescent complex (DNA Hoechst assay, see Supporting Information for details). The corresponding assays were applied on in vitro cultures after exposure to the thoroughly characterized nanoparticle dispersions for 3 or 6 days. The influence of concentration was tested for exposure to 0, 3.75, 7.5, and 15 parts per million (ppm, corresponds to microgram nanoparticles per milliliter) for 6 day periods or 0, 7.5, 15, and 30 ppm for 3 days exposure.

* Corresponding author e-mail: wendelin.stark@chem.ethz.ch; phone: +41 44 632 09 80; fax: +41 44 633 10 83.

† This paper is part of a focus group on Effects of Nanomaterials.

‡ ETH Zurich.

§ EMPA Materials Science and Technology.

10.1021/es052069i CCC: $33.50
Published on Web 03/11/2006

TABLE 1. Physical Properties of Investigated Nanoparticles

	SSA[a] m^2g^{-1}	density ρ 10^3 kg m^{-3}	d_{BET}[b] nm	d_{XDC}[c] nm	σ_G[d]	>200 nm[e] wt %	n_p[f]	sol.[g] $\mu g\ g^{-1}$	ref
reference materials									
crocidolite	8.5[i]	2.8−3.6				100		insol.	
SiO_2	191	2.2	14					insol.	*27, 28*
slightly soluble materials									
$Ca_3(PO_4)_2$	92	3.14	21	34	1.39	4	2	25	*27, 29*
Fe_2O_3	93	5.25	12	50	1.42	20	13	0.8	*27, 30*
ZnO	57	5.6	19	36	1.38	3	3	4.2[h]	*27, 31*
insoluble materials									
CeO_2	124	7.65	6	19	1.49	7	8	insol.	*27, 22*
TiO_2	188	4.23	8	20	1.27	< 1	5	insol.	*27, 32*
ZrO_2	96	5.63	11	20	1.43	11	3	insol.	*27*

[a] Specific surface area, errors ± 3%. [b] Particle size calculated from the specific surface area. [c] Hydrodynamic particle size as measured by X-ray disk centrifugation. [d] Geometric standard deviation (*33*, *34*). [e] Weight fraction of particles bigger than 200 nm. [f] Number of particles per hard agglomerate. [g] Solubility in water under standard conditions. [h] At 18 °C. [i] As supplied by the National Research Institute for Occupational Diseases, Johannesburg, South Africa.

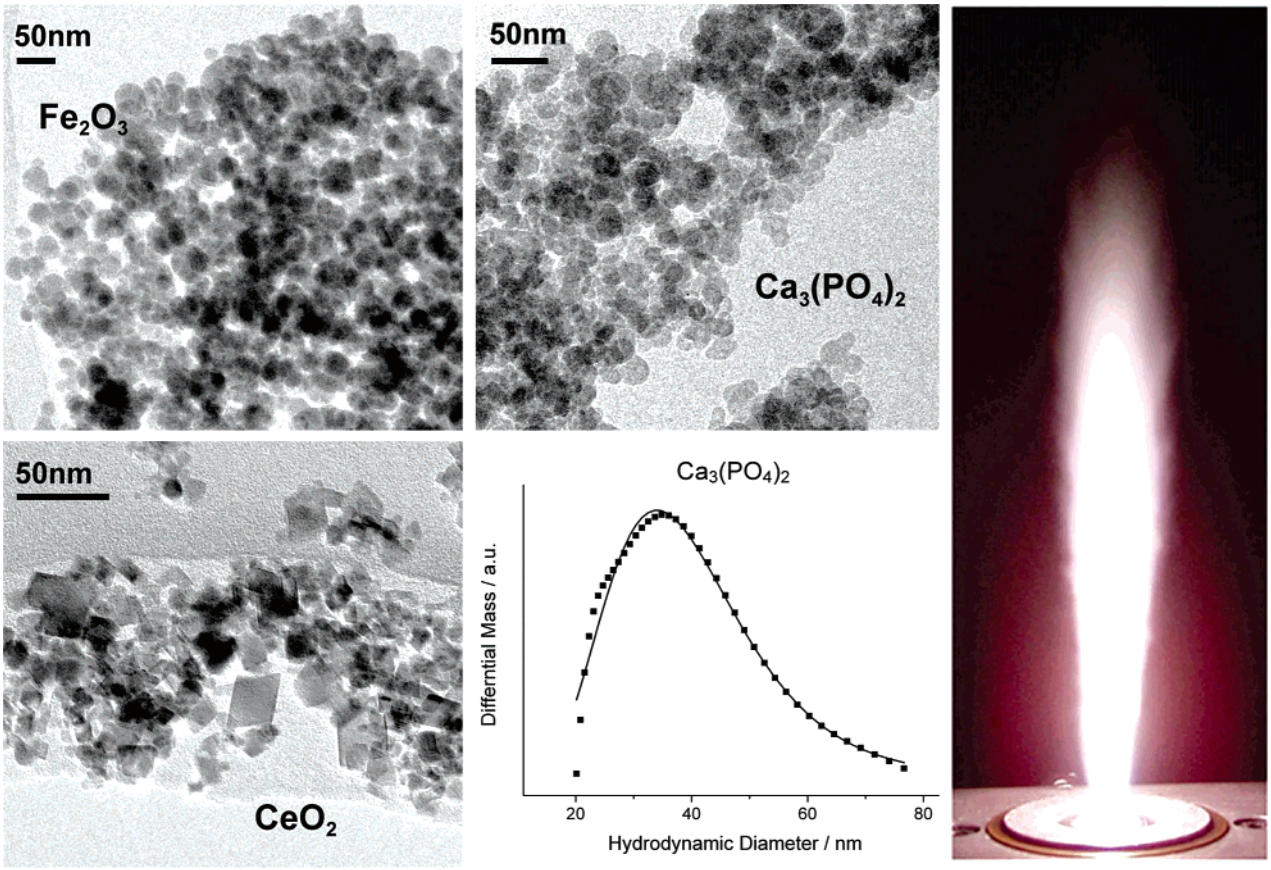

FIGURE 1. (left) Transmission electron microscopy images of selected nanoparticles after synthesis. Primary particles of 10−50 nm differ in terms of shape and degree of agglomeration. While iron oxide (Fe_2O_3) and tricalcium phosphate ($Ca_3(PO_4)_2$) contain small agglomerates of spherical particles, ceria (CeO_2) consists of irregular, mainly agglomerated nanoparticles. (middle, bottom) Measured (squares) and calculated (line) particle size distribution of tricalcium phosphate. (right) Flame synthesis of zirconia nanoparticles.

Results

Physical Properties. The physical properties of as-prepared nanoparticle dispersions are summarized within Table 1 listing the BET specific surface area measured by nitrogen adsorption, the density, the mean particle diameter d_{BET} assuming spherical particles and the solubility in water. Since the cytotoxicity of nanoparticles was evaluated using particle dispersions in aqueous solution, i.e., cell culture medium, the hydrodynamic particle diameter was consistently used throughout the present study as a measure for particle size and measured by X-ray disk centrifugation (XDC) (*25*, *26*). The corresponding mass-mean hydrodynamic particle size diameters d_{XDC} and the geometric standard deviation σ_g were included for comparison.

A representative full particle size distribution of tricalcium phosphate is given in Figure 1 and corroborates the good agreement with a fitted distribution to measured values. Additional full-size distributions of investigated materials are given in the Supporting Information. The mean number of primary particles per agglomerate n_p is included to account

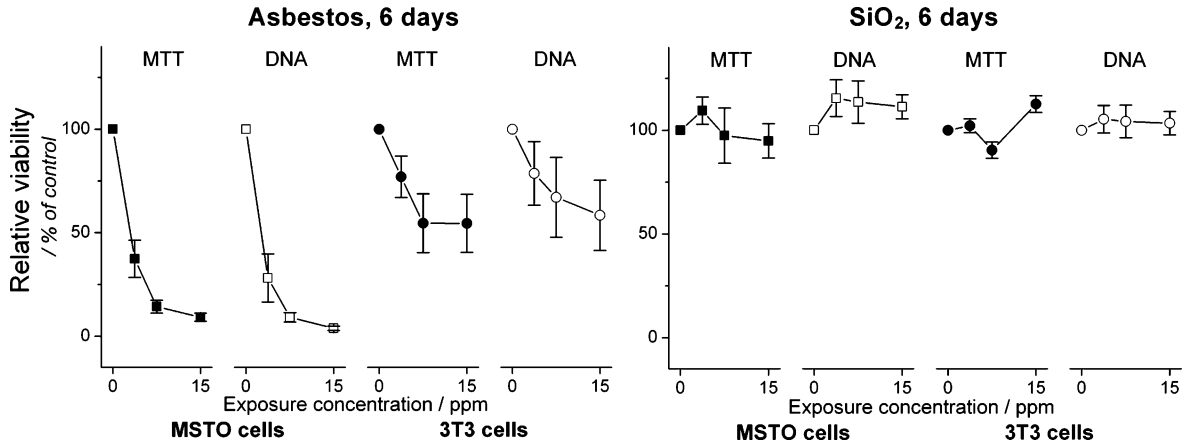

FIGURE 2. Effects of crocidolite (positive control) and silica (negative control) on MSTO and 3T3 cell cultures after 6 days treatment using 0−15 ppm (μg particles per mL culture medium). The high cytotoxicity of asbestos resulted in a pronounced drop of overall cell culture activity and strongly reduced DNA content.

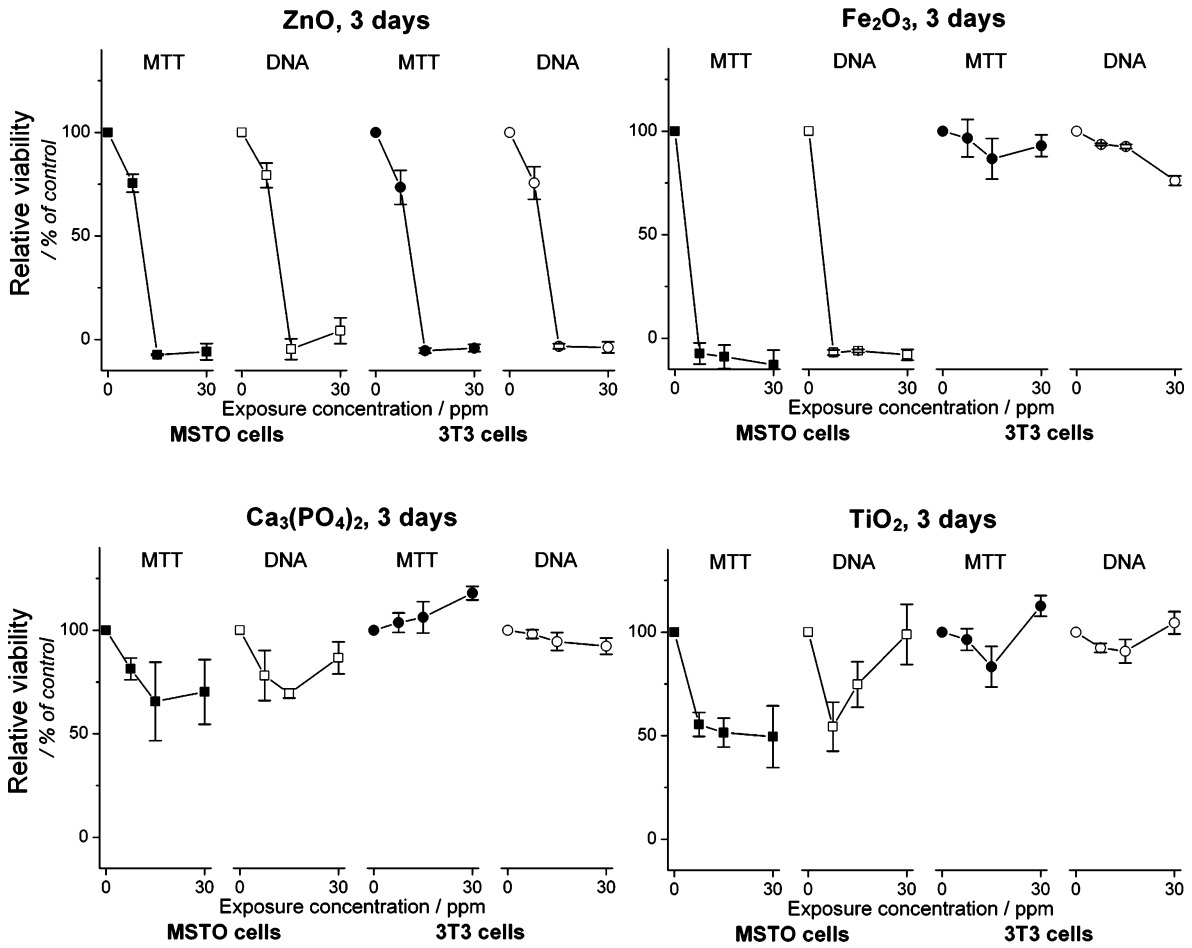

FIGURE 3. Effect of various slightly soluble nanoparticles on total cell culture MTT-conversion and DNA content after 3 days of treatment. For comparison, the data on cultures exposed to insoluble, yet biocompatible titania (right, bottom) after 3 days were included.

for hard agglomerates (*35*), e.g., in the case of iron oxide. Morphology and size of investigated materials are further shown in Figure 1 depicting representative transmission electron microscopy (TEM) images.

The estimated primary particle size from TEM qualitatively correlates to the calculated values d_{BET} and the mass-mean hydrodynamic particle diameter d_{XDC} (Table 1). The particle size distributions can be described as log-normal with geometric standard deviations ranging from 1.2 to 1.5 which is consistent with aggregation models for flame synthesis (*33*, *34*, *36*). The corresponding hydrodynamic agglomerate diameters are generally bigger than the calculated primary particle diameters d_{BET} corroborating the presence of small agglomerates (*25*). The average number of primary particles per aggregate (n_p) was roughly estimated (*25*) using the fractal scaling relationship ($n_p = [d_c/d_p]^D$) using d_{BET} as primary particle diameter (d_p), d_{XDC} as collision diameter (d_c), and a constant fractal dimension (D) of 1.8 consistent with theory for nanoparticle formation in flames (*37*) and measurements of aerosol-derived carbon black agglomerates (*38*).

Reference Materials and Exposure Concentrations. The relevant range of exposure concentrations was assessed using

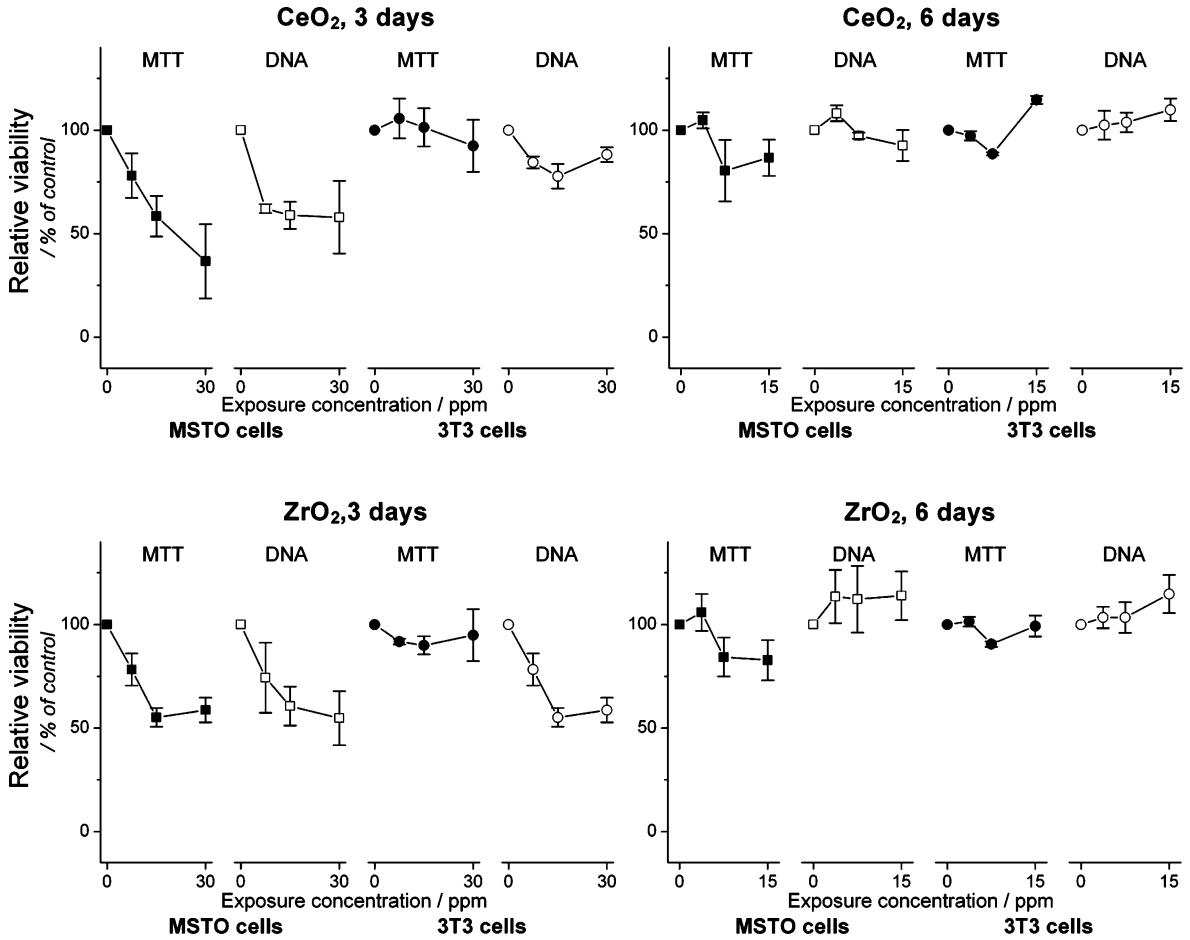

FIGURE 4. Exposure of ceria (CeO_2) or zirconia (ZrO_2) during 3 (left) or 6 days (right) resulted in distinctly different cell culture activity (MTT-conversion) and DNA contents. Both materials provoked a strong reaction for short exposure time but cultures mainly recovered after 6 days.

MSTO cells after treatment and based on a significant reduction of both cytotoxicity parameters in case of the positive control asbestos and the lack of effects using the negative control silica. For asbestos, a significant toxic effect was found at 3.75 ppm after 6 days or at 7.5 ppm after 3 days. No significant effects were observed for exposure to up to 15 ppm silica (see Figure 2) after 6 days and 30 ppm silica for 3 days.

To discuss the cytotoxicity of a set of industrially relevant nanoparticles with respect to silica or asbestos, particles were added to cell cultures at concentrations ranging from 3.75 to 15 ppm (6 day exposure period) and 7.5 to 30 ppm (3 day exposure period). The responses of cell cultures to silica and asbestos, respectively, are shown in Figure 2. The pronounced response of cells exposed to asbestos is reflected by loss of mean cell culture activity (full symbols) and decreased cell proliferation (open symbols).

Cytotoxicity of Slightly Soluble Nanoparticles. The exposure of cells to nanoparticles of zinc oxide, uncoated iron oxide, and tricalcium phosphate with a limited, yet detectable, solubility resulted in a pronounced response of the cell cultures to the nanoparticles. In the case of zinc oxide (ZnO) virtually all MSTO or 3T3 cells died after exposure to ZnO nanoparticle concentrations above 15 ppm (see Figure 3) as confirmed by light microscopy and biochemical parameters. Treatment of cell cultures with nanoparticulate uncoated iron oxide (Fe_2O_3) revealed a cell-type specific response. Slower proliferating 3T3 cells were only slightly affected by addition of up to 30 ppm iron oxide while the cell parameters MTT-conversion and DNA content of faster growing MSTO cells were drastically reduced upon exposure to as little as 3.75 ppm iron oxide. Both cell cultures seem to be able to deal with amorphous tricalcium phosphate in the investigated concentration range (0−30 ppm) which is in agreement with its broad use as implant material. No significant changes in 3T3 DNA quantity were observed following exposure to tricalcium phosphate; cell activity was even slightly increased. Human MSTO cells showed a small reduction of both cytotoxicity parameters at high concentration.

Cytotoxicity of Insoluble Nanoparticles. After exposure to insoluble ceria, titania, or zirconia, cell cultures showed a comparable response after 3 days where the values of the cell parameters were affected with increasing concentration. MSTO cells exhibited a higher sensitivity to the nanoparticles than 3T3 cells. Both cell activity and DNA content were significantly reduced by incubation with ceria and zirconia but cells were not completely killed even at high exposure concentrations (30 ppm). After 6 days the particle specific effects were not significant for 3T3 cells while the DNA assays revealed a significant but small increase in DNA content. More sensitive MSTO cells did not significantly change their cell activity for ceria and zirconia concentrations above 7.5 ppm, while the DNA quantity slightly increased as in the case of titania (Figure 3).

Cell Morphology. The pathogenesis of silicosis or asbestosis is characterized by the occurrence of odd-shaped fibroblasts and macrophages containing fiber remainders (*39*). Prior to strong changes in metabolism or proliferation, cells often change their shape in response to toxic reagents. The current study therefore routinely included light microscopic analysis of cell cultures. Figure 5A depicts normal

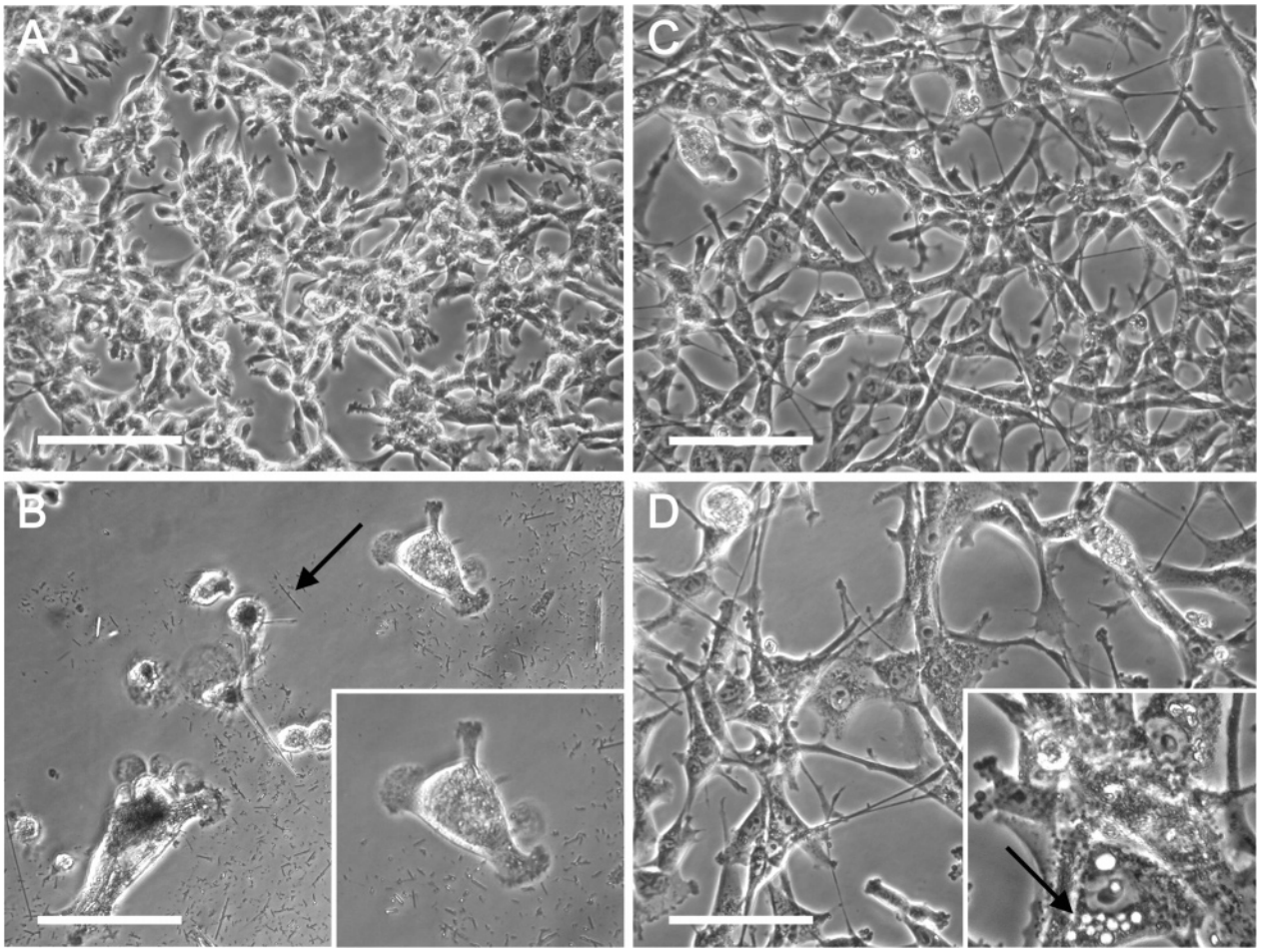

FIGURE 5. Morphological changes of MSTO cell cultures after 6 days incubation: (A) control cells without treatment; (B) 7.5 ppm crocidolite (see arrow for a single fiber), enlargement of a single cell which has increased in size, fibers surrounding the cell; (C) 7.5 ppm ZrO_2, no visible changes in morphology; (D) 15 ppm ZrO_2 resulting in the expression of small vesicles (probably apoptotic bodies, see arrow) in some cells. Scale bar 100 μm.

growing spindle-shaped MSTO cells in regular (no nanoparticles) cell culture medium. MSTO cells are fast growing (doubling time of ca. 18−24 h) and able to form multilayers. After 6 day incubation with 7.5 ppm crocidolite, all cells have undergone morphological changes to nearly spherical shape, gained in volume, and lost adhesion to the cell culture plate. Even higher concentrations of asbestos induced more dead cells. In contrast to asbestos, cells treated with 7.5 ppm ZrO_2 showed no visible morphological changes after 6 days of incubation. An increase of the concentration of ZrO_2 to 15 ppm provoked the formation of small vesicles (see enlargement) in some cells, probably apoptotic bodies.

Relative Cytotoxicity. A rough comparison of all materials for their cytotoxic response using MSTO (both MTT and DNA) after 3 days of treatment resulted in the following order: $Fe_2O_3 \approx$ asbestos > ZnO > $CeO_2 \approx ZrO_2 \approx TiO_2 \approx Ca_3(PO_4)_2$ which remained consistent for 6 day treatments. For 3T3 cells, reduced proliferation expressed as lower DNA content followed ZnO > asbestos $\approx ZrO_2 > Ca_3(PO_4)_2 \approx Fe_2O_3 \approx CeO_2 \approx TiO_2$ and showed an unexpected strong response of zirconia after 3 days exposure. The overall cell culture activity (MTT conversion) was drastically reduced for ZnO and asbestos while ZrO_2, $Ca_3(PO_4)_2$, Fe_2O_3, and CeO_2 were not much affected. After 6 days both 3T3 cytotoxicity parameters recovered for zirconia while cultures exposed to zinc and asbestos were irreversibly affected.

Discussion

Particle Characterization. Early investigations on the toxicity of nanosized materials have underlined the need for in-depth studies at physiologically relevant concentrations. The present study therefore investigated nanoparticles of different composition but similar size regarding their effects on living cells at concentrations ranging from 0 to 30 ppm. The inclusion of toxic asbestos and nontoxic amorphous silica permitted comparison of cytotoxic effects and showed that the investigated range of concentration is relevant to the comparison of oxide nanoparticles to asbestos fibers (Figure 2). The preparation and use of thoroughly characterized nanoparticles provides a base for data comparison and underlines the need for careful physical analysis of dispersions. A recent study by Soto et al. (*40*) investigated the cytotoxic response of nanostructured materials using a murine macrophage cell line. The investigated materials consisted of submicron (100 nm to 1 μm) or μm sized agglomerates only characterized by transmission electron microscopy. This visual method, however, does not yield reliable particle size data and gives a biased look at agglomeration and particle size distribution unless huge numbers of agglomerates are counted (*41*). The resulting toxicity data (EC 50 values) were nearly identical for most investigated compounds which is in sharp contrast to the present results. The use of a combination of quantitative analytical methods was found to be best adapted to deliver reliable size data of nanoparticle dispersions (*25*). A most recent study by Limbach et al. (*42*) on the in vitro agglomeration and uptake of nanoparticles at low concentrations has further revealed the crucial need for thorough particle size measurements of particle dispersions (*42*). Despite the inherent difficulties of transferring in vitro data

to in vivo scenarios, a test system should at least consider similar physical material properties. Untreated oxide nanoparticle dispersions undergo rapid agglomeration in cell culture medium (*42*). While in a given exposure scenario particles may differ in terms of agglomeration (size and form of soft agglomerates), they cannot be less agglomerated than in the procedure presented here: Highly characterized dispersions are mixed with cell culture medium just prior to exposure. In any other possible exposure method, the nanoparticles would also have to come into contact with a liquid phase at some point before contacting cells. Once entering this wet phase, rapid agglomeration inherently starts and uncoated oxide nanoparticles always form soft agglomerates if not stabilized by dispersion agents. The applied experimental procedure therefore models at least the worst case scenario of highly mobile, mainly unagglomerated nanoparticles coming in contact with a biological system. If investigating uncoated, nonmodified oxide nanoparticles as they are used in numerous applications, it is therefore not possible to differentiate between cytotoxicity arising from single or agglomerated nanoparticles since agglomeration is an inherent physical property of oxide nanoparticles in biological fluids.

Reference Materials. To provide suitable references on what may be considered toxic or acceptable, the current study used a specific type of asbestos and the food additive silica. Crocidolite, an amphibole form of asbestos, is insoluble and carcinogenic in humans and induces malignant mesothelioma. In cell culture, crocidolite evokes a profound decrease in cell functionality at low concentrations thus validating the presently used assays and cell lines. The cytotoxicity of crocidolite has been assigned to interactions with cell components after phagocytosis of the fibers (*43*, *44*). Since the fibers contain significant amounts of Fe, the influence of catalytic activity of the surface must be considered and motivates studies on catalytically active nanoparticles. The two investigated cell lines display different sensitivity to nanoparticles and underline the need for broader studies on the influence of specific cell properties on their response. It may be speculated that the higher sensitivity of MSTO compared to 3T3 cells could be attributed to a higher phagocytotic activity of MSTO cells resulting from their lower generation time. Faster growth results in a higher metabolic turnover and, as a consequence, more extracellular material is incorporated.

Effect of Particle Solubility. Toxic effects of nanoparticles may be attributed to two different actions: (*i*) a chemical toxicity based on the chemical composition, e.g., release of (toxic) ions and particle surface catalyzed reactions, e.g., formation of reactive oxygen species; or (*ii*) due to stress or stimuli caused by the surface, size and/or shape of the particles. It is not straightforward to differentiate between these two types of cytotoxicity, especially in the case when particles (partially) dissolve during culture treatment. The results on 7 different industrially relevant oxide nanoparticles (Figures 3−5) with two well established cell lines (one human, one rodent) confirmed that solubility greatly affected the cell culture response to the nanoparticles. Therefore it appears to be reasonable to group the different nanoparticles into slightly soluble and insoluble materials as suggested in Table 1.

Cytotoxicity of Soluble Oxide Nanoparticles. The lack of adverse effects following exposure to the biomaterial tricalcium phosphate (Figure 3) corroborates the use of the here-suggested cytotoxicity tests. A different behavior arises for zinc or iron oxide despite both being biologically most relevant trace elements. Zinc oxide, now used as a sunscreen ingredient (*45*), provoked a rapid drop of cell functionality at concentrations as low as 3.75 ppm (Figure 3). This toxic effect may be attributed to the release of Zn^{2+} ions before or after the uptake into the cell. The sharp concentration dependence of the cytotoxic response indicates the presence of a critical Zn^{2+} ion concentration in the culture medium and is in agreement with measurements on aqueous solutions of Zn^{2+}: The in vitro toxic concentration of $(Zn^{2+})_{aq}$ was reported around 400 μM (corresponding to 32 ppm ZnO) (*46*) or 10 ppm Zn^{2+} (*47*) while its mechanism is not well understood (*46*).

Cell cultures exposed to nanoparticles of uncoated iron oxide showed a cell-type specific response. Human MSTO cells were highly sensitive to Fe_2O_3 (see Figure 3) while rodent 3T3 cells were not greatly affected and remained viable throughout. Iron is known to be potentially toxic to cells at elevated concentration (*48*) and an investigation by Okeson et al. using rat alveolar epithelial cells revealed an EC_{50} of 4 mM Fe^{2+} (corresponds to 320 ppm Fe_2O_3) (*49*). The toxicity originates from the catalytic production of free radicals through Fenton and Haber−Weiss type reactions (*50*, *51*). The present results on uncoated iron oxide (Fe_2O_3) nanoparticles reveal a lethal concentration for MSTO cells above 7.5 ppm Fe_2O_3 nanoparticles. Assuming complete dissolution, a total $(Fe^{3+})_{aq}$ concentration of 94 μM would result in the culture medium of the present study. This value is about 40 times lower than the chemical toxicity of iron ions and therefore clearly demonstrates the presence of an additional nanoparticle specific cytotoxic effect. It may be speculated that the rapid uptake of nanoparticles (*42*) may transport the uncoated iron oxide into different compartments of the cell not normally accessed by aqueous iron ions.

Cytotoxicity of Insoluble Oxide Nanoparticles. Testing both a redox active (ceria, CeO_2, switching between Ce^{3+} and Ce^{4+}) and two redox inert (titania, TiO_2 and zirconia, ZrO_2) materials allowed a preliminary study on possible adverse effects of redox activity of insoluble materials. None of the insoluble materials was found to be exceedingly toxic up to 30 ppm. Yamamato et al. (*7*) evaluated the cytotoxicity of titania particles of different sizes and shapes and concluded IC_{50} results similar to thos found in this study. Both cell lines were able to better deal with nanoparticles when compared after exposure during 6 days instead of measurement after 3 days. It may be speculated that an initial stress arose from nanoparticle incorporation but sealing or detoxification of the nanoparticles in compartments may have helped to recover full cell culture viability. Such a sealing mechanism would agree with the results from Limbach et al. (*42*) who found that cells incorporate the ceria nanoparticles into vesicles. The formation of small vesicles (Figure 5) presumably containing part of the absorbed materials would agree with a mechanism where cells exclude the toxic intruders. The recovery of the cell culture stays in sharp contrast to the cytotoxicity of asbestos, the chemical toxicity of zinc oxide, or the particle-related toxicity of iron oxide where equal concentration-dependent sensitivity was found for 3 or 6 days exposure. More detailed investigations are needed to elucidate the mechanism of such recovery.

The comparison of cytotoxic effects from various nanoparticles sized similarly to silica and asbestos revealed a complex response that depends on measurement parameters, the duration of the treatment, and the type of cells. Particle solubility was found to be a suitable guiding parameter to group materials for their mainly chemical or physical effects. While slightly soluble zinc or iron oxide nanoparticles were relatively toxic, the effect of zinc could be attributed to a purely chemical effect of dissolved zinc ions. Iron oxide nanoparticles exhibited an astonishingly high toxicity that could not be explained by purely chemical effects of dissolved iron ions and thus indicates a nanoparticle-specific cytotoxic mechanism. Both redox active and inert, insoluble materials showed a clear cytotoxic effect for short exposure time and recovery after 6 days. In terms of particle solubility, acute

toxicological response arises from soluble materials and can be readily detected by a cell-based testing procedure. In contrast to this, nanoparticles of extremely low solubility will be persistent within the biological system and may provoke a range of long-term effects involving carcinogenic, mutagenic, or teratogenic influence on the organism. Therefore, degradable nanoparticles require a solid testing for acute toxicity while insoluble, persistent materials should additionally be assessed in terms of long-term toxic effects.

These results show that relatively simple cell culture MTT conversion and DNA content tests can be useful assays to make comparative statements on different nanoparticles if particles were thoroughly characterized prior to exposure. While the validity of in vitro results for in vivo situations is very limited, cytotoxic measurements provide at least a readily available early test system and may be suggested for prescreening nanoparticles. However, such simple tests are not sufficient to elucidate the molecular mechanisms underlying the observed adverse effects of specific particles. The complexity of nanoparticle-related cytotoxicity underlines the need for more detailed studies. In this respect, detailed examinations using advanced cell and molecular biological tests are required. Such investigations on a broader set of different cell lines combined with an understanding of the detailed molecular mechanism of nanoparticle cell interactions and comparison to in vivo experiments can then be used to develop a standardized pre-screening test for early toxicity assessment of nanoparticles.

Acknowledgments

We thank Dr. F. Krumeich for transmission electron microscopy images of the nanoparticles. Financial support by the ResOrtho and the Gebert Rüf Foundation, grant number GRS-048/04, is kindly acknowledged.

Supporting Information Available

Materials and Methods. This material is available free of charge via the Internet at http://pubs.acs.org.

Literature Cited

(1) Rittner, M. N. Market analysis of nanostructured materials. *Am. Ceram. Soc. Bull.* **2002**, *81*, 33−36.
(2) Service, R. F. Is Nanotechnology Dangerous? *Science* **2000**, *290*, 1526−1527.
(3) Warheit, D. B.; Laurence, B. R.; Reed, K. L.; Roach, D. H.; Reynolds, G. A. M.; Webb, T. R. Comparative pulmonary toxicity assessment of single-wall carbon nanotubes in rats. *Toxicol. Sci.* **2004**, *77*, 117−125.
(4) Oberdorster, G.; Sharp, Z.; Atudorei, V.; Elder, A.; Gelein, R.; Kreyling, W.; Cox, C. Translocation of inhaled ultrafine particles to the brain. *Inhal. Toxicol.* **2004**, *16*, 437−445.
(5) Colvin, V. The potential environmental impact of engineered nanomaterials. *Nat. Biotechnol.* **2003**, *21*, 1166−1170.
(6) Takeuchi, T.; Nakajima, M.; Morimoto, K. A human cell system for detecting asbestos cytogenotoxicity in vitro. *Mutat. Res.* **1999**, *438*, 63−70.
(7) Yamamoto, A.; Honma, R.; Sumita, M.; Hanawa, T. Cytotoxicity evaluation of ceramic particles of different sizes and shapes. *J. Biomed. Mater. Res.* **2004**, *68A*, 244−256.
(8) Maloney, W. J.; Smith, R. L.; Castro, F.; Schurman, D. J. Fibroblast Response to Metallic Debris in-Vitro − Enzyme-Induction, Cell-Proliferation, and Toxicity. *J. Bone Joint Surg. Am.* **1993**, *75A*, 835−844.
(9) Okazaki, Y.; Rao, S.; Asao, S.; Tateishi, T.; Katsuda, S.; Furuki, Y. Effects of Ti, Al and V concentrations on cell viability. *Mater. Trans. JIM* **1998**, *39*, 1053−1062.
(10) Hart, G. A.; Hesterberg, T. W. In vitro toxicity of respirable-size particles of diatomaceous earth and crystalline silica compared with asbestos and titanium dioxide. *J. Occup. Environ. Med.* **1998**, *40*, 29−42.
(11) Wottrich, R.; Diabate, S.; Krug, H. F. Biological effects of ultrafine model particles in human macrophages and epithelial cells in mono- and co-culture. *Int. J. Hyg. Environ. Health* **2004**, *207*, 353−361.
(12) Oberdorster, G.; Oberdorster, E.; Oberdorster, J. Nanotoxicology: An emerging discipline evolving from studies of ultrafine particles. *Environ. Health Perspect.* **2005**, *113*, 823−839.
(13) LeGeros, R. Z. Properties of osteoconductive biomaterials: calcium phosphates. *Clin. Orthop. Relat. Res.* **2002**, 81−98.
(14) Jarcho, M. Calcium-Phosphate Ceramics as Hard Tissue Prosthetics. *Clin. Orthop. Relat. Res.* **1981**, 259−278.
(15) Alexiou, C.; Jurgons, R.; Schmid, R.; Erhardt, W.; Parak, F.; Bergemann, C.; Iro, H. Magnetic Drug Targeting − A new approach in locoregional tumortherapy with chemotherapeutic agents. Experimental animal studies. *HNO* **2005**, *53*, 618−622.
(16) Berry, C. C.; Curtis, A. S. G. Functionalisation of magnetic nanoparticles for applications in biomedicine. *J. Phys. D: Appl. Phys.* **2003**, *36*, R198−R206.
(17) Gould, P. Nanoparticles probe biosystems. *Mater. Today* **2004**, *7*, 36−43.
(18) Gupta, A. K.; Gupta, M. Synthesis and surface engineering of iron oxide nanoparticles for biomedical applications. *Biomaterials* **2005**, *26*, 3995−4021.
(19) Jain, T. K.; Morales, M. A.; Sahoo, S. K.; Leslie-Pelecky, D. L.; Labhasetwar, V. Iron oxide nanoparticles for sustained delivery of anticancer agents. *Mol. Pharm.*. **2005**, *2*, 194−205.
(20) Schulze, E.; Ferrucci, J. T.; Poss, K.; Lapointe, L.; Bogdanova, A.; Weissleder, R. Cellular Uptake and Trafficking of a Prototypical Magnetic Iron-Oxide Label in-Vitro. *Invest. Radiol.* **1995**, *30*, 604−610.
(21) Pankhurst, Q. A.; Connolly, J.; Jones, S. K.; Dobson, J. Applications of magnetic nanoparticles in biomedicine. *J. Phys. D: Appl. Phys.* **2003**, *36*, R167−R181.
(22) Madler, L.; Stark, W. J.; Pratsinis, S. E. Flame-made ceria nanoparticles. *J. Mater. Res.* **2002**, *17*, 1356−1362.
(23) Stark, W. J.; Madler, L.; Maciejewski, M.; Pratsinis, S. E.; Baiker, A. Flame synthesis of nanocrystalline ceria-zirconia: effect of carrier liquid. *Chem. Commun.* **2003**, 588−589.
(24) Mosmann, T. Rapid colorimetric assay for cellular growth and survival: Application to proliferation and cytotoxicity assays. *J. Immunol. Methods* **1983**, *65*, 55−63.
(25) Staiger, M.; Bowen, P.; Ketterer, J.; Bohonek, J. Particle size distribution measurement and assessment of agglomeration of commercial nanosized ceramic particles. *J. Dispersion Sci. Technol.* **2002**, *23*, 619−630.
(26) Mcfadyen, P.; Fairhurst, D. High-Resolution Particle-Size Analysis from Nanometers to Microns. *Clay Miner.* **1993**, *28*, 531−537.
(27) Perry, H.; Green, D.; Maloney, O. *Perry's Chemical Engineers' Handbook*, 7th ed.; McGraw-Hill: New York, 1997.
(28) Briesen, H.; Fuhrmann, A.; Pratsinis, S. E. The effect of precursor in flame synthesis of SiO_2. *Chem. Eng. Sci.* **1998**, *53*, 4105−4112.
(29) Loher, S.; Stark, W. J.; Maciejewski, M.; Baiker, A.; Pratsinis, S. E.; Reichardt, D.; Maspero, F.; Krumeich, F.; Günther, D. Fluoroapatite and calcium phosphate nanoparticles by flame synthesis. *Chem. Mater.* **2005**, *17*, 36−42.
(30) Cornell, R.; Schwertmann, U. *The Iron Oxides: Structure, Properties, Reactions, Occurrences and Uses*; Wiley-VCH Verlag GmbH: Weinheim, 2003.
(31) Madler, L.; Stark, W.; Pratsinis, S. Rapid synthesis of stable ZnO quantum dots. *J. Appl. Phys.* **2002**, *92*, 6537−6540.
(32) Stark, W. J.; Pratsinis, S. E.; Baiker, A. Flame made titania/silica epoxidation catalysts. *J. Catal.* **2001**, *203*, 516−524.
(33) Dekkers, P. J.; Friedlander, S. K. The self-preserving size distribution theory I. Effects of the Knudsen number on aerosol agglomerate growth. *J. Colloid Interface Sci.* **2002**, *248*, 295−305.
(34) Vemury, S.; Pratsinis, S. E. Self-Preserving Size Distributions of Agglomerates. *J. Aerosol Sci.* **1995**, *26*, 175−185.
(35) Friedlander, S. K. *Smoke, Dust and Haze*; Oxford University Press: Oxford, 2000.
(36) Grass, R. N.; Stark, W. J. Flame synthesis of calcium-, strontium-, barium fluoride nanoparticles and sodium chloride. *Chem. Commun.* **2005**, 1767−1769.
(37) Kruis, F. E.; Kusters, K. A.; Pratsinis, S. E.; Scarlett, B. A Simple-Model for the Evolution of the Characteristics of Aggregate Particles Undergoing Coagulation and Sintering. *Aerosol Sci. Technol.* **1993**, *19*, 514−526.
(38) Katrinak, K. A.; Rez, P.; Perkes, P. R.; Buseck, P. R. Fractal geometry of carbonaceous aggregates from an urban aerosol. *Environ. Sci. Technol.* **1993**, *27*, 539−547.
(39) Bowden, D. H.; Adamson, I. Y. R. The Role of Cell Injury and the Continuing Inflammatory Response in the Generation of Silicotic Pulmonary Fibrosis. *J. Pathol.* **1984**, *144*, 149−161.
(40) Soto, K. F.; Carrasco, A.; Powell, T. G.; Garza, K. M.; Murr, L. E. Comparative in vitro cytotoxicity assessment of some manu-

factured nanoparticulate materials characterized by transmission electron microscopy. *J. Nanopart. Res.* **2005**, *7*, 145−169.
(41) Tsantilis, S.; Kammler, H. K.; Pratsinis, S. E. Population balance modeling of flame synthesis of nanoparticles. *Chem. Eng. Sci.* **2002**, *57*, 2139−2156.
(42) Limbach, L. K.; Li, Y. C.; Grass, R. N.; Brunner, T. J.; Hintermann, M. A.; Muller, M.; Gunther, D.; Stark, W. J. Oxide nanoparticle uptake in human lung fibroblasts: Effects of particle size, agglomeration, and diffusion at low concentrations. *Environ. Sci. Technol.* **2005**, *39*, 9370−9376.
(43) Liu, W. H.; Ernst, J. D.; Broaddus, V. C. Phagocytosis of crocidolite asbestos induces oxidative stress, DNA damage, and apoptosis in mesothelial cells. *Am. J. Respir. Cell Mol. Biol.* **2000**, *23*, 371−378.
(44) Garcia, J. G. N.; Gray, L. D.; Dodson, R. F.; Callahan, K. S. Asbestos-Induced Endothelial-Cell Activation and Injury − Demonstration of Fiber Phagocytosis and Oxidant-Dependent Toxicity. *Am. Rev. Respir. Dis.* **1988**, *138*, 958−964.
(45) Pinnell, S. R.; Fairhurst, D.; Gillies, R.; Mitchnick, M. A.; Kollias, N. Microfine zinc oxide is a superior sunscreen ingredient to microfine titanium dioxide. *Dermatol. Surg.* **2000**, *26*, 309−314.
(46) Palmiter, R. D. Protection against zinc toxicity by metallothionein and zinc transporter 1. *Proc. Natl. Acad. Sci., U.S.A.* **2004**, *101*, 4918−4923.
(47) Borovansky, J.; Riley, P. A. Cytotoxicity of Zinc In vitro. *Chem-Biol. Interact.* **1989**, *69*, 279−291.
(48) Jacobs, A.; Worwood, M. *Iron in Biochemistry and Medicine II*; Academic Press: New York, 1980.
(49) Okeson, C. D.; Riley, M. R.; Riley-Saxton, E. In vitro alveolar cytotoxicity of soluble components of airborne particulate matter: effects of serum on toxicity of transition metals. *Toxicol. in Vitro* **2004**, *18*, 673−680.
(50) Symons, M. C. R.; Gutteridge, J. M. C. *Free Radicals and Iron: Chemistry, Biology, and Medicine*; Oxford University Press: Oxford, 1998.
(51) Nunez, M. T.; Garate, M. A.; Arredondo, M.; Tapia, V.; Munoz, P. The cellular mechanisms of body iron homeostasis. *Biol. Res.* **2000**, *33*, 133−142.

Received for review October 19, 2005. Revised manuscript received January 6, 2006. Accepted February 2, 2006.

ES052069I